



Evidence for “dark charge” from photoluminescence measurements in wide InGaN quantum wells

A. BERCHA,¹ W. TRZECIAKOWSKI,^{1,*}  G. MUZIOL,¹ J. W. TOMM,²  AND T. SUSKI¹

¹*Instytut Wysokich Ciśnień PAN, Sokołowska 29/37, 01-142 Warsaw, Poland*

²*Max-Born-Institut, Max-Born-Str. 2A, D-12489 Berlin, Germany*

*[wt@unipress.waw.pl](mailto:wtr@unipress.waw.pl)

Abstract: Wide (15-25 nm) InGaN/GaN quantum wells in LED structures were studied by time-resolved photoluminescence (PL) spectroscopy and compared with narrow (2.6 nm) wells in similar LED structures. Using below-barrier pulsed excitation in the microsecond range, we measured increase and decay of PL pulses. These pulses in wide wells at low-intensity excitation show very slow increase and fast decay. Moreover, the shape of the pulses changes when we vary the separation between them. None of these effects occurs for samples with narrow wells. The unusual properties of wide wells are attributed to the presence of “dark charge” i.e., electrons and holes in the ground states. Their wave functions are spatially separated and due to negligible overlap they do not contribute to emission. However, they screen the built-in field in the well very effectively so that excited states appear with significant overlap and give rise to PL. A simple model of recombination kinetics including “dark charge” explains the observations qualitatively.

Published by Optica Publishing Group under the terms of the [Creative Commons Attribution 4.0 License](https://creativecommons.org/licenses/by/4.0/). Further distribution of this work must maintain attribution to the author(s) and the published article's title, journal citation, and DOI.

1. Introduction

InGaN/GaN light emitting diodes (LEDs) form the basis of white light emitters and their properties have been examined in numerous aspects [1,2]. Typically, the LEDs are grown on c-plane of hexagonal wurtzite structures, which causes the well-known limitations originating from strong built-in electric fields [3]. In particular, in the quantum wells the electron and hole states become separated by the quantum-confined Stark effect (QCSE) [4]. To limit the detrimental consequence of low wavefunction overlap, the QWs were rather narrow (2-4 nm). Escapes from this bottleneck have been sought, in particular, by growing on semipolar or nonpolar surfaces [5–8]. However, this leads to lower structural quality of the devices. Other attempts to reduce the negative effects of QCSE consisted in growing staggered quantum wells [9]. However, a technologically much simpler way of eliminating the built-in field using the well-established growth on c-plane is to move to wider wells (10-25 nm). There, the observed radiative recombination significantly increases compared to the conventional wells [10–14]. The reason for this is the efficient screening of built-in field by electrons and holes, which occupy the widely separated ground states E_1 and H_1 (localized at the opposite edges of the well). The light emission occurs from transitions between the excited states (E_2 and H_2 or higher), which extend over a large portion of the well and have significant overlap (Fig. 1). Since the charge in the ground states cannot recombine radiatively, we will refer to it as “dark charge”, while the observed increased emission seems to be due solely to excited state transitions. However, even if the “dark charge” in ground states does not contribute to the photoluminescence (PL) or electroluminescence (EL) it can still affect optical properties of the structure. In [15], we have shown anomalies in photocurrent, which were attributed to the charge in the ground states.

In the present paper, we give experimental evidence for the presence of “dark charge” in the wells by comparing the PL from narrow and from wide wells. Pulsed measurements reveal some important properties of these structures that cannot be obtained from CW studies.

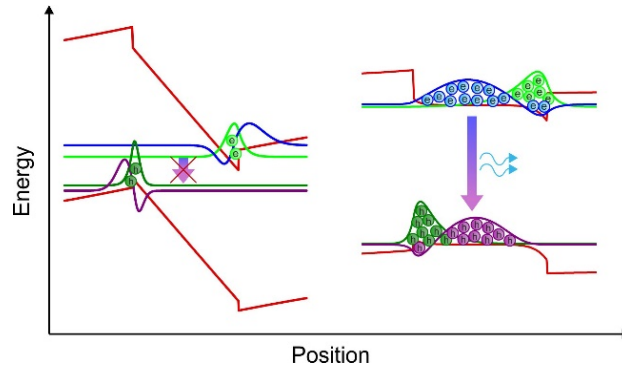


Fig. 1. Potential profile in a wide InGaN/GaN quantum well for low injection (left) and for high injection (right). At low injection, large field separates electrons and holes in ground and in excited states, so that no recombination is possible. At high injection, charge in the ground states (“dark charge”) remains close to the edges of the well and screens the built-in field. This leads to increased overlap of excited states and to efficient emission.

For the present study we used a special set of samples with $\text{In}_{0.02}\text{Ga}_{0.98}\text{N}$ barriers and $\text{In}_{0.17}\text{Ga}_{0.83}\text{N}$ wells, allowing resonant excitation of QWs at 405 nm and PL emission in the range of 440–480 nm. By generating carriers directly in the well we eliminate the transport and capture effects which occur for above-barrier excitation.

In case of time-resolved PL, we studied not only the decay of the signal after excitation (like in typical experiments using sub picosecond excitation [16–19]) but also the evolution of the emission (both the spectra and intensity) during the laser pulse (in the microsecond range). Since we expect the decay of the “dark charge” to be very slow, we also measured the PL pulses as a function of their separation up to 30 milliseconds. These results show the effects due to “dark charge” in wide wells, compared to properties of standard narrow wells. In the theoretical section we present a model which shows how the “dark charge” may affect radiative recombination dynamics. In concert, this gives a picture of the behavior of the “dark charge” in device structures with wide wells. These results also stimulate the anticipation that c-plane grown LEDs and diode lasers with wide QWs will provide a real quality boost in device development.

2. Samples and experimental details

The diodes were grown by plasma-assisted molecular beam epitaxy on bulk c-plane n-GaN substrates. The full profile of Samples I, II and III is shown in Fig. 2. First, a 100 nm GaN:Si (Si: $2 \times 10^{18} \text{ cm}^{-3}$) is grown, followed by a 40 nm thick $\text{In}_{0.02}\text{Ga}_{0.98}\text{N}$ lower barrier and an $\text{In}_{0.17}\text{Ga}_{0.83}\text{N}$ well. The thickness of the QW is 2.6, 15, 25 nm in Samples I, II and III, respectively. Next, the 20 nm $\text{In}_{0.02}\text{Ga}_{0.98}\text{N}$ upper barrier, 20 nm $\text{Al}_{0.13}\text{Ga}_{0.87}\text{N}:\text{Mg}$ (Mg: $2 \times 10^{19} \text{ cm}^{-3}$) electron blocking layer (EBL) and 200 nm GaN:Mg (Mg: $5 \times 10^{18} \text{ cm}^{-3}$) were placed. The tunnel junction consisting of 10 nm $\text{In}_{0.02}\text{Ga}_{0.98}\text{N}:\text{Mg}$ (Mg: $3 \times 10^{19} \text{ cm}^{-3}$), 2.5 nm $\text{In}_{0.24}\text{Ga}_{0.76}\text{N}:\text{Mg}$ (Mg: $1 \times 10^{20} \text{ cm}^{-3}$), 2.5 nm $\text{In}_{0.24}\text{Ga}_{0.76}\text{N}:\text{Si}$ (Si: $1 \times 10^{20} \text{ cm}^{-3}$) and 10 nm $\text{In}_{0.02}\text{Ga}_{0.98}\text{N}:\text{Si}$ (Si: $3 \times 10^{19} \text{ cm}^{-3}$) was grown so as to have n-type GaN:Si on top. Such n-type layer has good conductivity so that the contacts cover only a small part of the upper surface. The diodes were processed into squares $0.35 \times 0.35 \text{ mm}$. We also grew Samples IV and V which contained only a single $\text{In}_{0.17}\text{Ga}_{0.83}\text{N}$ well 25 and 2.6 nm wide, respectively, with undoped $\text{In}_{0.02}\text{Ga}_{0.98}\text{N}$ barriers

(no p-n junction, no electron-blocking layer or tunnel junction) which were used as reference samples to make sure that the observed effects were not due to these additional layers in the structure.

100nm GaN:Si
Tunnel junction
200nm GaN:Mg
20 nm $\text{Al}_{0.15}\text{Ga}_{0.85}\text{N:Mg}$ EBL
20 nm $\text{In}_{0.02}\text{Ga}_{0.98}\text{N}$
d_{qw} $\text{In}_{0.17}\text{Ga}_{0.83}\text{N}$ QW
40 nm $\text{In}_{0.02}\text{Ga}_{0.98}\text{N}$
100 nm GaN:Si
bulk GaN c-plane substrate

Fig. 2. Profile of our LED with tunnel junction. Samples I, II and III are identical but the thickness of the quantum well (d_{QW}) is 2.6, 15 and 25 nm, respectively.

PL spectra were excited by the 405 nm laser diode, the spot diameter on the sample was about 50 μm . The emission passed through a SPEX1000M monochromator and was recorded with a Hamamatsu photomultiplier (with photon counting) using a narrow time gate when studying PL pulses. The diode laser driven by pulsed power supply typically shows some power and wavelength instability due to heating. Therefore, the most reliable way to generate short rectangular pulses was to operate the laser diode in Continuous Wave (CW) mode and use an acousto-optic modulator as fast shutter. The rise and fall times of our excitation pulses were around 50 ns. We varied the excitation pulse length from 1 μs up to 1000 μs and the time gate of the photomultiplier was selected between 10 ns up to 1 μs to measure the time evolution of the PL pulse with sufficient accuracy. We also measured the PL spectra at different time positions during the pulse. For low-intensity excitation these measurements took several hours. It turned out that the PL was sensitive not only to the duration and peak power of the exciting laser, but also to the distance between the pulses. Therefore, we varied the separation between the pulses from 3 μs up to 30 ms. Results shown in the present paper were obtained at room temperature.

3. PL results for narrow and for wide wells

For CW excitation there are significant differences between narrow and wide wells. In Fig. 3 we show the power dependence of the PL spectra. The emission intensities are compared in Fig. 4 and the emission wavelengths in Fig. 5.

The emission from narrow well starts at lower excitation power and for low powers is much stronger than the emission from wide wells. Only for high excitation the wide wells “catch up”.

The emission wavelengths for samples I, II, and III obtained from PL (EL) spectra are shown in Fig.5a (Fig.5b). We observe a 10-15 nm blue shift for the narrow well, most likely due to screening of the field by photoexcited electrons and holes. There is almost no wavelength shift for the wide wells. Similar results have been obtained in previous papers [12–14]. This suggests that

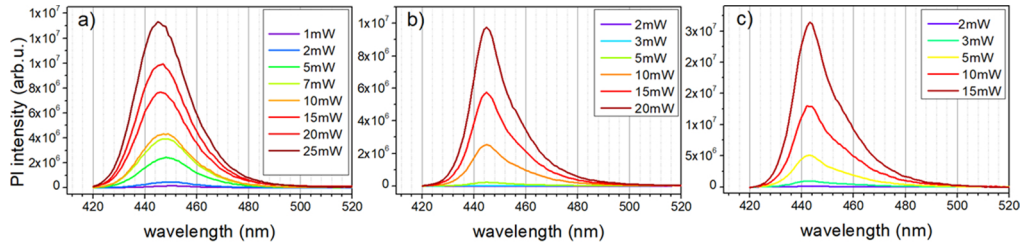


Fig. 3. Examples of PL spectra for: a) sample I (2.6 nm well), b) sample II (15 nm well) and c) sample III (25 nm well) for different excitation powers.

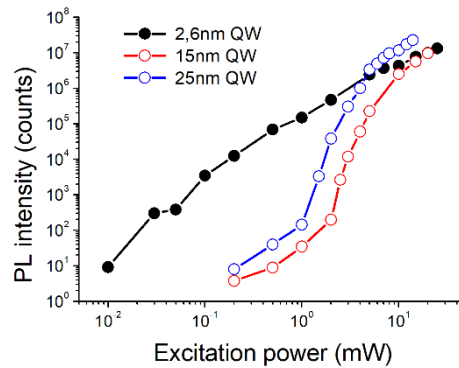


Fig. 4. Power dependence of PL intensity from narrow (Sample I, black circles) and wide (sample II, red circles, Sample III, blue circles) quantum wells. (CW excitation at 405 nm).

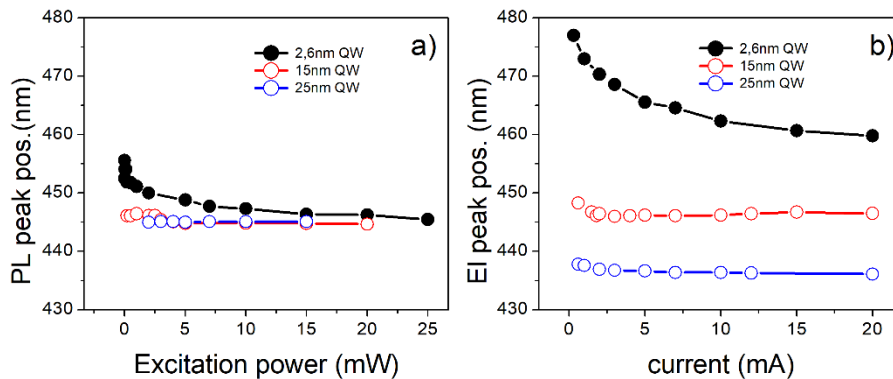


Fig. 5. Emission wavelengths for narrow (black circles), and for wide (red and blue circles) wells as a function of excitation power obtained from PL peaks (a) and from EL peaks (b) for CW excitation.

as soon as the wide well starts to emit light, the electric field in the well is almost fully screened (see Fig. 1); the emission intensity changes with excitation power but the emission wavelength remains stable, which implies a stable electric field in the well. Additional experiments involving hydrostatic pressure [20], indicate that the field is close to zero. It is also interesting that for the wide well the EL and PL wavelengths are fairly close while for the narrow well the EL wavelengths are about 15-20 nm longer than the PL wavelengths. This is due to the fact that EL emission occurs for stronger electric field in the well (increased by the forward voltage). For wide wells the field is screened regardless of the applied voltage.

Let us now turn to pulsed excitation. In Fig. 6 we show PL excited by 30 μs long 405 nm laser pulses for Sample I (2.6 nm quantum well) for different excitation powers. We can see that the pulses are rectangular (in the μs time range) for all excitation powers. There is no measurable delay between the excitation pulse and the PL pulse. The pulses did not change while we varied their separation. The PL spectra showed 10 nm blue shift with increasing power similarly to the CW case shown in Fig. 5.

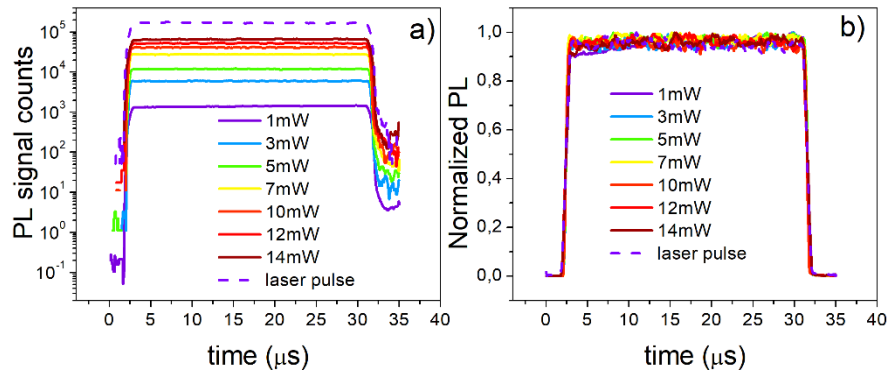


Fig. 6. PL from Sample I (2.6 nm well) under pulsed excitation for different excitation powers: intensity in log scale (a) and in linear scale, normalized (b).

All the above properties of InGaN narrow wells have been studied in detail as a function of voltage, temperature, etc.; they are well known and are presented here for reference. Meanwhile, the results of similar measurements for structures with wide wells are very different.

In Fig. 7 a,b we show PL for several excitation powers (405 nm excitation, 30 μs duration, 10% fill factor) for Sample III. For high-power excitation the PL response is rectangular but for low powers, the increase of PL signal is extremely slow (we compare the PL of Sample I and Sample III in Fig.7c). Moreover, for low laser powers there is some delay between the laser pulse and the onset of PL signal.

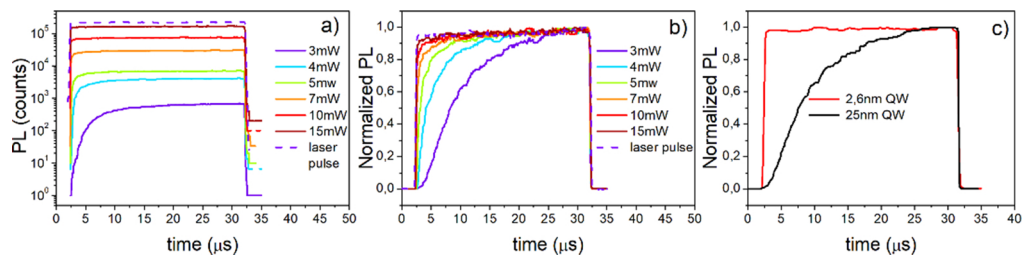


Fig. 7. PL for the 30- μs , 405-nm excitation of sample III by different powers (10% fill factor), (a) in logarithmic scale, (b) normalized in linear scale, (c) comparison of the normalized PL signals for sample I and sample III at 3 mW excitation.

In the next step we varied the separation between the pulses to check if they “interact” i.e., if the shape of individual PL pulse depends on the time interval between the pulses. Therefore, in Fig. 8 we compare the shape of the 30- μ s pulses for fixed excitation at 405 nm (7 mW power) but as a function of time interval between the pulses (i.e., of the fill factor). Both the speed of the rise and the final intensity of the pulse is affected by the temporal separation between them. Only when the time interval between pulses was sufficiently large, we observed that the PL signal did not depend on it. In case of shorter time interval, the “dark charge” is present from the previous pulse and it affects the PL signal. In case of 7-mW excitation the limit of “isolated” pulse seems to be achieved at about 3 ms separation. This confirms that in wide quantum wells there are slow processes affecting the PL emission, most probably slow decay of “dark charge”.

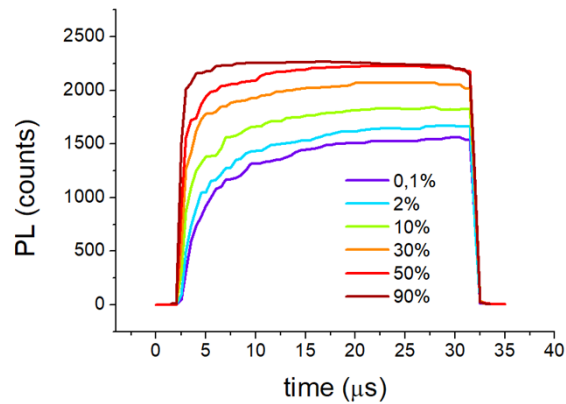


Fig. 8. The effect of different spacing (fill factor) of 30 μ s pulses (sample II, spacing from 3.3 μ s to 29970 μ s) for excitation power of 7 mW.

Another test revealing the presence of “dark charge” between the pulses is shown in Fig. 9. Five microseconds after the PL excitation pulse a short (1 μ s) negative voltage pulse was applied. Negative (reverse) voltage should reduce the electric field in the well, thus facilitating thermal escape of “dark charge” and the reappearance of (optically active) excited states [21]. In Fig. 9 we observe indeed light emission accompanying the negative voltage pulse. Moreover, a change in the shape of the PL signal dependent on the negative voltage level can be seen, similar to the

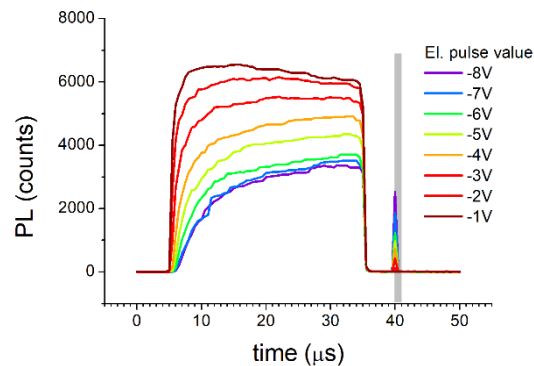


Fig. 9. The effect of short (1 μ s) reverse-voltage pulses on PL pulses from Sample II excited by 7 mW, 405 nm, 30 μ s laser pulse (fill factor 10%). The voltage pulse is applied 5 μ s after the end of PL excitation and is marked with a grey shade. The reverse voltage is varied from -1 V to -8 V. Apart from the voltage pulse, the sample is biased at 0 V.

changes observed for varying fill factor shown in Fig. 8. We can see a reduction of intensity and increased rise time of the PL signal for increased negative voltage pulse. We attribute this to reduction of the population of “dark charge” by the applied negative voltage.

Those unusual properties of wide wells will be modeled in the next section.

4. Theory

The PL from an InGaN/GaN quantum well depends on many factors: one has to account for screening of the field in the well (which depends on carrier concentration), calculate carrier losses due to thermal emission or tunneling, nonradiative recombination (both Shockley-Reed-Hall and Auger), include bimolecular and excitonic mechanism etc. Here we would like to examine the effect of “dark charge” on PL in wide wells using a simplified model. First, we assume that the screening occurs almost instantaneously and the PL emission from wide well occurs at negligible electric field, regardless of the power or duration of the excitation pulse. This is justified by the fact that the emission line does not shift with power or time during the pulse. The electrons and holes in their ground states are screening the electric field very effectively since there is practically no overlap of their wavefunctions, i.e., the “dark charge” is close to the opposite edges of the well. This means that radiative and nonradiative recombination of the “dark charge” can be neglected. The emission occurs when the carriers start to populate the excited states, which have a significant overlap [12] and recombine both radiatively and nonradiatively. We consider only one excited state E_2 (and H_2) although there will be many more excited states with significant overlap. The two-dimensional concentration of electrons in the ground state with energy E_1 can be written as

$$n_1 = \left(\frac{kTm^*}{\pi\hbar^2} \right) \ln \left[1 + \exp \left(\frac{E_F - E_1}{kT} \right) \right], \quad (1)$$

and the concentration of electrons in the excited state E_2

$$n_2 = \left(\frac{kTm^*}{\pi\hbar^2} \right) \ln \left[1 + \exp \left(\frac{E_F - E_2}{kT} \right) \right], \quad (2)$$

where E_F is the quasi Fermi level dependent on excitation power and on time, m^* is the effective mass. If we neglect the recombination of “dark charge” n_1 and consider only the Shockley-Reed-Hall (SRH) and bimolecular recombination of n_2 , we obtain a simple kinetic equation

$$\frac{d}{dt}(n_1 + n_2) = P_a - An_2 - B_r(n_2)^2, \quad (3)$$

where P_a is the concentration of carriers pumped into the well (per unit time) by the excitation beam (or by the current in case of EL), A is the SRH recombination rate and B_r is the radiative recombination rate. P_a is proportional to the power of the excitation, but only a small fraction of the incident photons is absorbed in the well. P_a also includes the possible contribution of photocurrent (i.e., escape of carriers from the well by tunneling or thermal excitation). Photocurrent is usually proportional to the excitation power so it will lead to an effectively lower P_a . We neglect here the Auger recombination, since the concentration in the excited state n_2 will be relatively small (compared to n_1). We also neglect the excitonic recombination and we assume that the concentration of holes will be identical to that of electrons. Our main goal is to show that the presence of n_1 in Eq.(3) may significantly change the dynamics of PL emission.

It is convenient to introduce the function $y(t)$

$$y(t) = \exp \left(\frac{E_F - E_2}{kT} \right), \quad (4)$$

and the parameter

$$g = \exp\left(\frac{E_2 - E_1}{kT}\right) \quad (5)$$

so that

$$n_1 = \left(\frac{kTm^*}{\pi\hbar^2}\right) \ln[1 + gy], \quad (6)$$

and

$$n_2 = \left(\frac{kTm^*}{\pi\hbar^2}\right) \ln[1 + y], \quad (7)$$

The parameter g depends on the separation between the ground state and the excited state (and on temperature). When we insert Eqs. (6) and (7) into Eq. (3) we obtain a simple equation for $y(t)$

$$\left[\frac{g}{1+gy} + \frac{1}{1+y}\right] \frac{dy}{dt} = P - A \times \ln(1+y) - B \times [\ln(1+y)]^2, \quad (8)$$

where $P = \left(\frac{\pi\hbar^2}{kTm^*}\right) \times P_a$, $B = \left(\frac{kTm^*}{\pi\hbar^2}\right) \times B_r$. If we assume Boltzmann statistics for the excited state E_2 we can replace $\ln(1+y)$ by y in Eq.(8). It then becomes an Abel equation and we can separate the variables and integrate it analytically. However, this leads to formulas for $t(y)$ instead of $y(t)$. It is easier to solve Eq.(8) numerically for a given set of parameters A , B , P and g . Please note that when we set $g = 0$ in Eq.(6) we obtain $n_1 = 0$ i.e. the case without “dark charge”. The initial condition for $y(t)$ is chosen so that at $t = 0$ both n_1 and n_2 are very small, e.g. $y(0) = \exp(-10)$. In Fig. 10 we plot the values of $[\ln(1+y)]^2$ (proportional to $(n_2)^2$ and to PL intensity) calculated from Eq.(8) for $A = 10 \mu\text{s}^{-1}$, $B = 20 \mu\text{s}^{-1}$, $P = 1 \mu\text{s}^{-1}$ and three values of g .

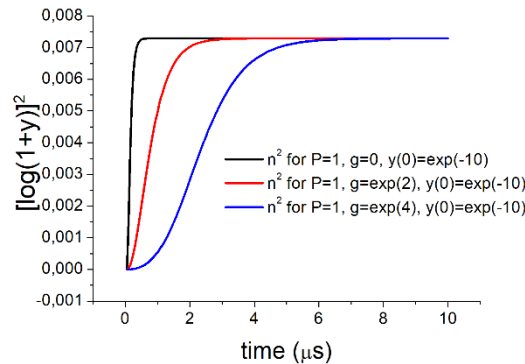


Fig. 10. Onset of the PL pulse (arb. units) for $g = 0$ (no “dark charge”), for $g = \exp(2)$, and for $g = \exp(4)$ i.e. for increasing $(E_2 - E_1)/kT$. The excitation power P is fixed at $1 \mu\text{s}^{-1}$.

We can see that the contribution of “dark charge” slows the increase of the pulse significantly and that this effect is stronger for increasing $(E_2 - E_1)/kT$. Therefore, we can expect the effect of “dark charge” to increase at low temperature, since $E_2 - E_1$ should not change much with temperature. However, both A and B depend on temperature (typically A increases and B decreases with increasing temperature [18]).

In Fig. 11 we show the onset of PL pulses for increasing excitation power P . For low excitation the delay of the PL signal with respect to the excitation pulse is large and it takes more time to reach saturation (steady state). This corresponds to the experimental results shown in Fig. 7.

We can also use Eq.(8) for modeling the decay of the PL pulse (i.e. for $P = 0$) assuming some initial value of $y(0)$. In Fig. 12 we show the full $10 \mu\text{s}$ pulse determined from Eq.(8) (i.e. both the

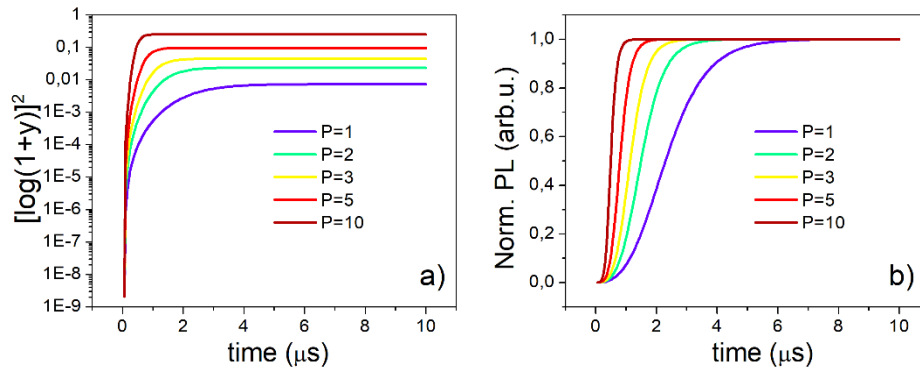


Fig. 11. Onset of the PL pulse (arb. units) for $g = \exp(4)$ and increasing excitation power P (in μs^{-1}) (a) logarithmic scale, (b) linear scale for normalized values.

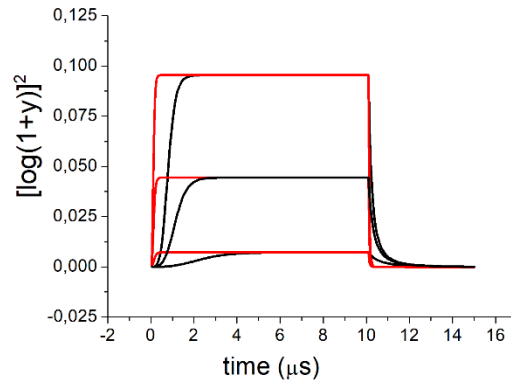


Fig. 12. PL pulse for $g = 0$ (red curves) and for $g = \exp(4)$ (black curves) at three values of excitation power ($P = 1 \mu\text{s}^{-1}$, $P = 3 \mu\text{s}^{-1}$, and $P = 5 \mu\text{s}^{-1}$).

increase, saturation and decay). The effect of “dark charge” ($g \neq 0$) is most pronounced for low excitation powers. The slow decay of the pulses was not observed experimentally (Fig. 7).

This is the main discrepancy between the simple theory and the experiment which shows (for low intensity excitation) a slow increase but a rapid decrease of the PL pulse. The reason for fast decay could be the tunneling out of the well due to strong field in the barrier (tunneling is not included in our simple model).

5. Conclusions

Wide InGaN/GaN quantum wells reveal some unexpected physical effects which we attribute to the presence of “dark charge” occupying the ground states in the well and separated spatially so that this charge does not contribute to PL or EL emission. However, this “dark charge” affects the emission due to excited states through slowing the increase of the PL signal and causing some “interaction” between the pulses. The presence of “dark charge” in-between the PL pulses is also revealed by reverse-voltage pulses. Simple kinetic model agrees qualitatively with some of the observed anomalies in PL.

Funding. Narodowe Centrum Nauki (2019/35/D/ST3/03008); Narodowe Centrum Badań i Rozwoju (LIDER/35/0127/L9/17/NCBR/2018); Horizon 2020 Research and Innovation Program (MBI002741); Laserlab-Europe.

Disclosures. The authors declare no conflicts of interest.

Data availability. Data underlying the results presented in this paper are not publicly available at this time but may be obtained from the authors upon reasonable request.

References

1. S. Nakamura, "Nobel Lecture: Background story of the invention of efficient blue InGaN light emitting diodes," *Rev. Mod. Phys.* **87**(4), 1139–1151 (2015).
2. M. R. Krames, O. B. Shchekin, R. Mueller-Mach, G. O. Mueller, L. Zhou, G. Harbers, and M. G. Craford, "Status and Future of High-Power Light-Emitting Diodes for Solid-State Lighting," *J. Disp. Technol.* **3**(2), 160–175 (2007).
3. F. Bernardini, V. Fiorentini, and D. Vanderbilt, "Spontaneous polarization and piezoelectric constants of III-V nitrides," *Phys. Rev. B* **56**(16), R10024 (1997).
4. V. Fiorentini, F. Bernardini, F. Della Sala, A. Di Carlo, and P. Lugli, "Effects of macroscopic polarization in III-V nitride multiple quantum wells," *Phys. Rev. B* **60**(12), 8849–8858 (1999).
5. F. Scholz, "Semipolar GaN grown on foreign substrates: a review," *Semicond. Sci. Technol.* **27**(2), 024002 (2012).
6. M. Funato and Y. Kawakami, "Excitonic properties of polar, semipolar, and nonpolar InGaN/GaN strained quantum wells with potential fluctuations," *J. Appl. Phys.* **103**(9), 093501 (2008).
7. D. F. Feezell, J. S. Speck, S. P. DenBaars, and S. I. Nakamura, "Semipolar (2021) InGaN/GaN Light-Emitting Diodes for High-Efficiency Solid-State Lighting," *J. Disp. Technol.* **9**(4), 190–198 (2013).
8. Y. Enya, Y. Yoshizumi, T. Kyono, K. Akita, M. Ueno, M. Adachi, T. Sumitomo, S. Tokuyama, T. Ikegami, K. Katayama, and T. Nakamura, "531 nm Green Lasing of InGaN Based Laser Diodes on Semi-Polar $\{20\bar{2}1\}$ Free-Standing GaN Substrates," *Appl. Phys. Express* **2**, 082101 (2009).
9. H. Zhao, G. Liu, J. Zhang, J. Dierolf, and N. Tansu, "Approaches for high internal quantum efficiency green InGaN light-emitting diodes with large overlap quantum wells," *Opt. Express* **19**(S4), A991 (2011).
10. N. F. Gardner, G. O. Müller, Y. C. Shen, G. Chen, S. Watanabe, W. Götz, and M. R. Krames, "Blue-emitting InGaN–GaN double-heterostructure light-emitting diodes reaching maximum quantum efficiency above 200A/cm²," *Appl. Phys. Lett.* **91**(24), 243506 (2007).
11. A. Laubsch, W. Bergbauer, M. Sabathil, M. Strassburg, H. Lugauer, M. Peter, T. Meyer, G. Brüderl, J. Wagner, N. Linder, K. Streubel, and B. Hahn, "Luminescence properties of thick InGaN quantum-wells," *Phys. Status Solidi C* **6**(S2), S885–S888 (2009).
12. G. Muziol, H. Turski, M. Siekacz, K. Szkudlarek, L. Janicki, M. Baranowski, S. Zolud, R. Kudrawiec, T. Suski, and C. Skierbiszewski, "Beyond Quantum Efficiency Limitations Originating from the Piezoelectric Polarization in Light-Emitting Devices," *ACS Photonics* **6**(8), 1963–1971 (2019).
13. G. Muziol, M. Hajdel, M. Siekacz, H. Turski, K. Pieniak, A. Bercha, W. Trzeciakowski, R. Kudrawiec, T. Suski, and C. Skierbiszewski, "III-nitride optoelectronic devices containing wide quantum wells - unexpectedly efficient light sources," *Jpn. J. Appl. Phys.* **61**(SA), SA0801 (2022).
14. M. Hajdel, M. Chlipała, M. Siekacz, H. Turski, P. Wolny, K. Nowakowski-Szkudlarek, A. Feduniewicz-Żmuda, C. Skierbiszewski, and G. Muziol, "Dependence of InGaN Quantum Well Thickness on the Nature of Optical Transitions in LEDs," *Materials* **15**(1), 237 (2022).
15. A. Bercha, W. Trzeciakowski, G. Muziol, M. Siekacz, and C. Skierbiszewski, "Anomalous photocurrent in wide InGaN quantum wells," *Opt. Express* **28**(4), 4717 (2020).
16. P. Lefebvre, S. Kalliakos, T. Bretagnon, P. Valvin, T. Taliercio, B. Gil, N. Grandjean, and J. Massies, "Observation and modeling of the time-dependent descreening of internal electric field in a wurtzite GaN/Al_{0.15}Ga_{0.85}N quantum well after high photoexcitation," *Phys. Rev. B* **69**(3), 035307 (2004).
17. Wolf-Alexander Quitsch, Daniel Sager, Moritz Loewenich, Tobias Meyer, Berthold Hahn, and Gerd Bacher, "Low injection losses in InGaN/GaN LEDs: The correlation of photoluminescence, electroluminescence, and photocurrent measurements," *J. Appl. Phys.* **123**(21), 214502 (2018).
18. Andreas Hangleiter, "Recombination dynamics in GaInN/GaN quantum wells," *Semicond. Sci. Technol.* **34**(7), 073002 (2019).
19. Aurelien David, Nathan G. Young, Cory Lund, and Michael D. Craven, "The Physics of Recombinations in III-Nitride Emitters," *ECS J. Solid State Sci. Technol.* **9**(1), 016021 (2020).
20. Katarzyna Pieniak, Witold Trzeciakowski, Grzegorz Muziol, Anna Kafar, Marcin Siekacz, Czesław Skierbiszewski, and Tadeusz Suski, "Evolution of a dominant light emission mechanism induced by changes of the quantum well width in InGaN/GaN LEDs and LDs," *Opt. Express* **29**(25), 40804 (2021).
21. Ulrich T. Schwarz, H. Braun, K. Kojima, Y. Kawakami, S. Nagahama, and T. Mukai, "Interplay of built-in potential and piezoelectric field on carrier recombination in green light emitting InGaN quantum wells," *Appl. Phys. Lett.* **91**(12), 123503 (2007).